

Imaging and visualization of complex nematic fields

Slobodan Žumer^{*a,b}

Miha Čančula^a, Simon Čopar^{a,b}, Miha Ravnik^a

^aFaculty of Mathematics and Physics, University of Ljubljana, Slovenia

^bJozef Stefan Institute, Slovenia

* slobodan.zumer@fmf.uni-lj.si; <http://softmatter.fmf.uni-lj.si>

ABSTRACT

Modeling and experiments on nematic ordering in geometrically frustrated nematic and chiral nematic systems reveals diverse birefringent micro and sub-micro structures, including knotted and linked nematic braids, skyrmions, torons, and hopfions. Here, these complex defect structures are used to illustrate simulations of optical images and visualization of complex nematic fields. Particular attention is given to simulations of images obtained by three-photon excitation fluorescence polarizing microscopy that can unveil complex three dimensional nematic fields at the micrometer scale.

Keywords: Director field, Q-tensor nematic field, splay, bend & twist deformations, topological defects, singular defects, nonsingular defects, nematic braids, torons, hopfions, knots, polarization microscopy, Pontryagin-Thom surface, three-photon fluorescence polarizing microscopy.

1. INTRODUCTION

Complex geometrical constraints and intrinsic chirality in nematic mesophases allow for formation of stable and metastable defect structures of high complexity. Recently knots and links of arbitrary kind have been formed using laser micro-manipulation of nematic braids entangling colloidal particles in nematic liquid crystals [1]. In frustrated chiral nematic phases stable and metastable toron and hopfion defects have been implemented by laser tweezers [2,3]. Complex colloidal particles in the form of platelets, handle-bodies, and knots have led to intricate yet controllable nematic fields [4-6]. In numerical studies we predicted numerous exotic structures in confined blue phases [7,8] and stable knotted disclinations in cholesteric droplets with homeotropic boundary conditions [9]. Moebius type colloidal particles were shown to directly induce knotted disclinations in simple nematics [10]. Modeling studies based on the numerical minimization of the phenomenological free energy, supported with the adapted topological theory [11-14] allow for a rather straightforward study and characterization of the diverse structures. Crucial for the understanding of the nematic structures is the visualization of the ordering fields [15]. Here, we review some recently observed and predicted complex defect and nematic-field structures using different visualization approaches for their presentation. The numerically obtained structures are also used to simulate polarization microscopy (PM) images and micrographs that are obtained with three-photon fluorescence PM for selected types of polarization [16]. Finally, this paper is a contribution towards predictable-design of complex soft materials with possible use in advanced complex optics and photonics.

2. DESCRIPTIONS OF NEMATIC ORDERING FIELDS

The director field is the central and most commonly used parameter to describe the orientational ordering of nematic liquid crystals. It is often used for approximate analytic and simplified numerical modeling. Formally, the possible states

of the director constitute a unit sphere (director is a unit-length vector-field), with opposite directions describing the same physical state. Regions with an ill-defined orientational field are called topological defects. The studies of defects, based on the director profile, mostly focus on the topological properties of point defects and on the winding number of disclination lines. Such approaches can characterize elementary features in the director field through application of homotopy theory [17–20]. For point defects, topological charges are defined as integrals over the enclosing surfaces [19–22]. The disclinations are well described by their winding numbers, but in case they are closed, they also carry a topological charge [23,13]. Visualization is essential for understanding of the nematic defect structures. The recent surge of interest in complex nematic defect structures, often at submicron scales, requires approaches where beside topological quantities also geometrical aspects and fine details of ordering play an essential role. Therefore, instead of a simple director based description of the orientational molecular ordering in nematogenic materials, a spatially dependent tensorial order parameter Q_{ij} [24] based approach is used. This tensor “nematic field” is defined as a second moment of the orientational molecular distribution, $Q_{ij} = \langle 3a_i a_j / 2 - \delta_{ij} \rangle$, where a_i is a Cartesian coordinate of \mathbf{a} - the single molecule orientational vector, and the brackets denote the ensemble average. Usually it is written in the form

$$Q_{ij} = S(3n_i n_j - \delta_{ij})/2 + P e_i^+ e_j^+ / 2 - P e_i^- e_j^- / 2, \quad (1)$$

where the first term describes the average orientation of molecules along the director \mathbf{n} and scales with the well-known degree of orientational order S , whereas the second two terms describe biaxiality of the molecular orientational distribution [24]. The parameter P measures the degree of biaxiality of the field, discriminating the e^+ axis along which the fluctuations of the molecular orientation are largest, from the e^- axis along which the fluctuations are smallest. Degree of order S ranges from $-1/2$ to 1 , but in practice mostly stays positive, while P is in most areas practically zero. The equilibrium nematic field can be obtained by minimizing the model-form of the nematic free energy [24]. Note that relevant physical scales cover a broad range of values from several microns to only few nanometers. For smaller scales, molecular Monte Carlo and molecular dynamics approaches need to be used [25, 26]. On the experimental side, until recently, the conventional polarization microscopy has been practically the only tool for the determination of the nematic field. Measuring techniques improved with the evolution of precise fluorescence-based microscopy techniques [27-29]. By using multiple polarizations and detection of fluorescence signal, it is possible to determine the director field with submicron resolution in three spatial dimensions. In this way a three-dimensional director field can be reconstructed and visualized. The comparison of experimentally measured fields and predictions from modeling approaches can be used to improve weaknesses of the experimental reconstruction on one side and to adapt and improve the free-energy functional with all relevant terms for optimal prediction of the nematic field on the other hand [30].

2.1. GLYPHS, STREAMLINES AND POLARIZATION MICROSCOPY

In nematic liquid crystals simple director field is usually represented by line segments (Figure 1a). Unfortunately, effectively, this is useful only if visualizing inplane director fields which are twodimensional. The out-of-plane director on a two-dimensional cross section was traditionally described by ‘nails’, where the out-of plane orientation was marked by distinguishing the length of the nail (Figure1c). With the advances of computer graphics a straightforward method is to draw the director as glyphs of different shapes (Figure1 b&d) where shading is used to represent orientation. In case those deformations are rather weak or more complex in the third dimension, streamlines that follow director field are a better of visualization than glyphs. It should be stressed that its implementation requires careful use of tensorial nature of the director field taking into account the \mathbf{n} to $-\mathbf{n}$ symmetry of the director [15]. The approach with streamlines is illustrated by a visualizing the twisted boojums that accompany a colloidal particle with planar anchoring in a chromonic liquid crystal [18]. By comparing Figures 1e&f one clearly sees that glyphs hardly indicate the left & right twisting of the nematic

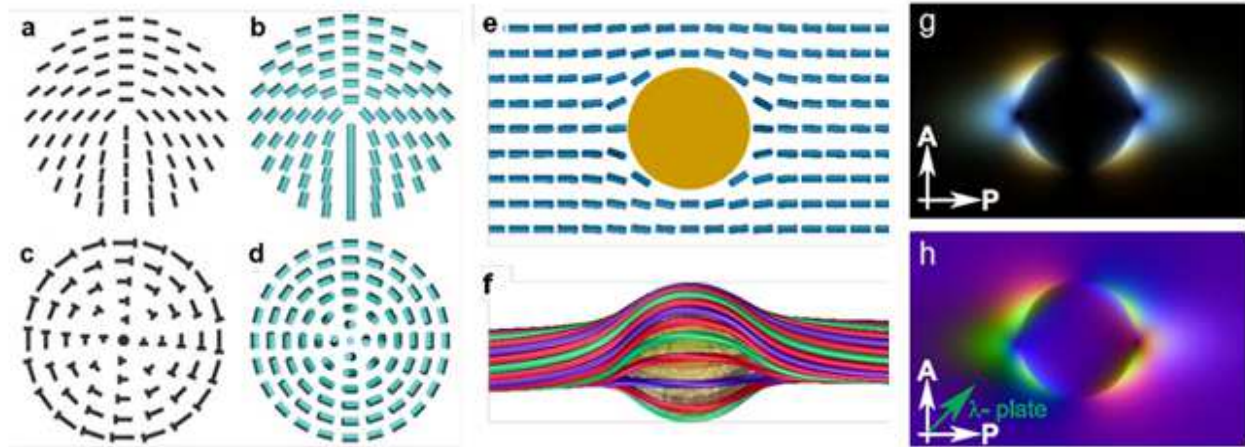


Figure 1: (a, b) Use of two kinds of glyphs for the presentation of 2D director fields in a cross section of a singular $+1/2$ disclination and (c,d) a nonsingular $+1$ twisted disclination. (e,f) Glyph presentation is contrasted to the stream lines for the case of counter-twisted boojums that accompany colloidal sphere enforcing planar anchoring in a chromonic liquid crystal. (g) Simulated polarization microscope picture of a director field induced by such a colloidal particle under crossed polarizers and (h) under crossed polarizers with added lambda plate.

director which on contrary is clearly seen in the streamline presentation. The director field glyphs enhanced by color coding are another option to better describe 3D variation of the nematic field [15].

Experimentally, the most common way of observing liquid crystalline structures is by polarized optical transmission microscopy (PM) (e.g. see Ref. 24). This method has a strong potential for recognition of structures primarily in cases when the structures vary mostly in a plane perpendicular to the observation direction. However, even for rather simple 3D nematic fields the method is much less effective in determining details of the structure. The method is also limited to samples that are thinner than the coherence length of the light. To obtain a simulated PM picture usually simple straight ray optics is used to calculate the total phase shift between ordinary and extraordinary component of the ray. The computation is based on slicing the Q-tensor field into long and thin prisms along which effectively, the light-ray is propagated. The local variation of birefringence is described by the Jones matrices [31]. This technique allows for calculations of a transmitted monochromatic and polychromatic light. The simulated white light PM pictures of a two opposite twisted boojums accompanying a planar colloidal particle in a chromonic liquid crystal (Figures 1g&h) demonstrate that beside microscopy with cross polarizers also a picture with inserted lambda wave plate is needed to uncover twisting details of such 3D nematic field [32].

2.2. DEGREE OF ORDER AND DISCLINATIONS

Defect structures are often visualized by plotting only singular defect lines via drawing isosurfaces of constant nematic degree of order S for some preselected value that is lower as in unperturbed bulk nematic [31, 33]. The Figure 2a illustrates a simple case of a homeotropic colloidal spherical particle encircled by a $-1/2$ disclination ring. The visualization of the disclination loop via S -isosurface is accompanied by line segment representation of the inplane director field. In contrast, for a trefoil knot-like homeotropic colloidal particle accompanied by two knotted disclination lines (Figure 2b) the director is intentionally omitted as it strongly varies in all three spatial dimensions (for details on the experiment and modeling see Ref. 6).

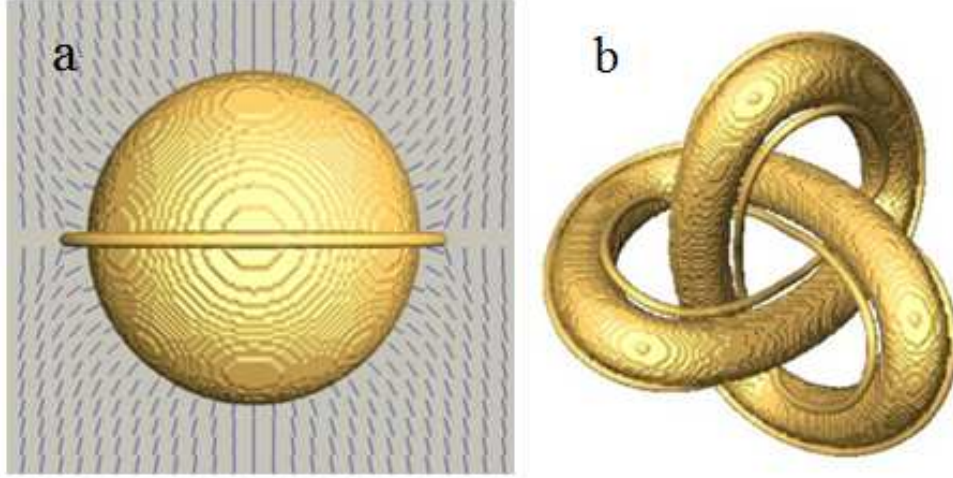


Figure 2: Presentation of the $-1/2$ singular disclination lines that accompany colloidal particles with homeotropic surface anchoring of a nematic media using isosurfaces of S corresponding to the 5% reduction of the bulk order parameter. The Saturn ring disclination loop which encircles the spherical colloidal particle is complemented also by the nematic director field in a cross section (a). In case of knotted colloidal particle, the physical knot is entangled by two nematic field knots (b). To avoid an overcrowded picture the director field is intentionally not presented.

2.3. SPLAY, BEND AND TWIST

To examine the fine structure of the director field around defects, the elastic nematic deformation modes -splay, bend and twist- can be effectively extracted and visualized by highlighting the degree of specific deformations in the immediate surroundings of the defects without showing complete nematic field. One such parameter that easily visualizes the winding number of disclination lines is the scalar splay-bend parameter S_{SB} , constructed from second derivatives of the order parameter tensor Q_{ij} [34]:

$$S_{SB} = \frac{\partial^2 Q_{ij}}{\partial x_i \partial x_j}, \quad (2)$$

where note that summation over repeated indices is assumed. Effectively, the scalar splay-bend parameter S_{SB} is fully analogous to the divergence of the order- and flexoelectric polarization arising from the deformation of the nematic field in a simplified flexoelectric model [24]. Neglecting the biaxiality and variation of the degree of order S , the tensor form reduces to the well-known vector form:

$$S_{SB} = \frac{3S}{2} \nabla \cdot (\mathbf{n}(\nabla \cdot \mathbf{n}) - \mathbf{n} \times (\nabla \times \mathbf{n})). \quad (3)$$

The first term stems from a strong divergence of splay deformation that corresponds to positive S_{SB} , while negative values of the second term imply strong divergence of the bend deformation. Splay-bend parameter visualization can be applied also for distorted director profiles, as long as the splay and bend deformations reach extremes nearby the disclination lines. The splay-bend parameter proves to be particularly efficient in finding escaped defect lines with integer winding numbers (see Ref. 15). When visualizing twist deformations in chiral and archiral nematic liquid crystals a local twist parameter S_{TW} , similar to the chiral term in the nematic elastic free-energy is used [8]:

$$S_{TW} = \varepsilon_{ikl} Q_{ij} \frac{\partial Q_{lj}}{\partial x_k} - \frac{9}{4} S^2 q_0, \quad (4)$$

where S is the bulk-order parameter and q_0 is the inverse pitch different from zero only for intrinsically chiral phases, making S_{TW} zero in the ground state of chiral and achiral nematics. It is convenient for identifying twist variations of

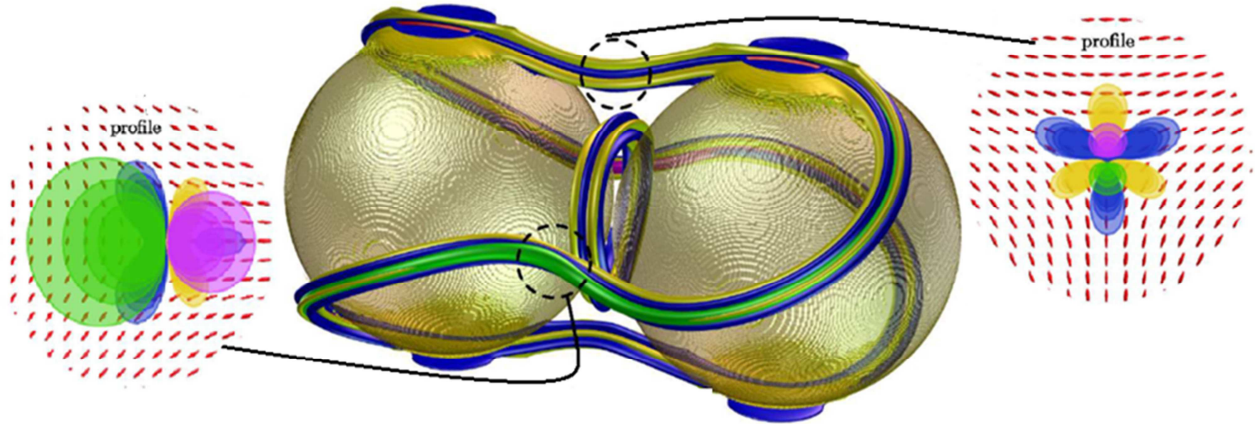


Figure 3: Colloidal dimer confined to π -twisted nematic cell is bound by a (small) circular $-1/2$ disclination loop and a larger more complex $-1/2$ disclination loop that locally notably deviates from the $-1/2$ hyperbolic, as visualized by the splay-bend parameter and twist parameter. Blue color indicates large splay and yellow large bend. Green and violet indicates positive and negative twisting. The two insets show local cross-sections of the larger loop.

singular disclination lines mostly induced by geometrical confinement and for twisted deformations of nonsingular disclinations when the anisotropy of the twist elastic constant (weak) plays the crucial role. For practical purposes both parameters are scaled with the nematic correlation length, thus being dimensionless quantities. Figure 3 illustrates how the splay-bend and twist parameters vary along a $-1/2$ disclination loop entangling a colloidal dimer in a π -twisted nematic cell [35]. In Figure 4 it is illustrated how the splay-bend parameter S_{SB} can reveal distortions of a $-1/2$ disclination loop in a cholesteric phase confined to a spherical droplet with the surface imposing strong homeotropic anchoring. The line cross-sections distort only close to the surface whereas in the bulk they exhibit geometrical distortions known as writhe and twist. The sum of writhe and twist equals the topological invariant – self-linking number - of an arbitrary complex $-1/2$ disclination loop [12,9].

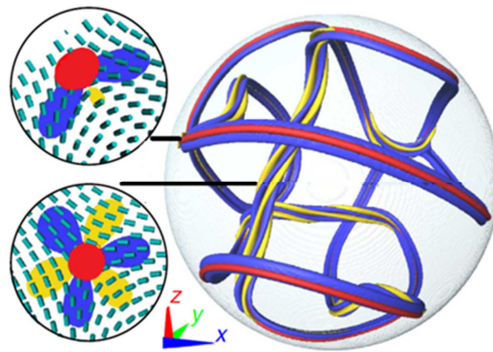


Figure 4: Knotted disclination loop in a cholesteric droplet with homeotropic surface anchoring. Diameter of the droplet is 5 times the value of the intrinsic cholesteric pitch. The splay-bend parameter and nematic order parameter are used to show that profile of the disclination which deviates substantially from the three-fold ribbon when near the surface of the droplet.

2.4. PONTRYAGIN–THOM SURFACE AND MULTI-PHOTON FLUORESCENCE POLARIZATION MICROSCOPY

The elementary polarization microscopy technique for 2D nematic structures based on counting dark Schlieren brushes was in past years extended to three dimensions by studying three-dimensional regions that share common director orientation, as can be determined by confocal multi-photon fluorescence polarization microscopy [27-29]. Chen and collaborators have shown [3,13] that by selecting the light beam direction, the Pontryagin – Thom (PT) surface can be constructed that is formed of points where director is perpendicular to the beam direction. The surface is particularly simple when the system is characterized by a homogenous far-field director and a beam that is parallel to it. The PT surface is closed for nematic fields that have no defects and no confining surfaces. In case of confinement, the PT surface is limited by confining isosurfaces and similarly, if defects are present, they also limit the PT surface. For more details how PT surfaces are linked to topological charges see Ref. 15. In Figure 5, the colloidal particle in a homogenous unwinded cholesteric farfield is decorated by a hopfion, making the PT surface simple yet bounded by the particle. The

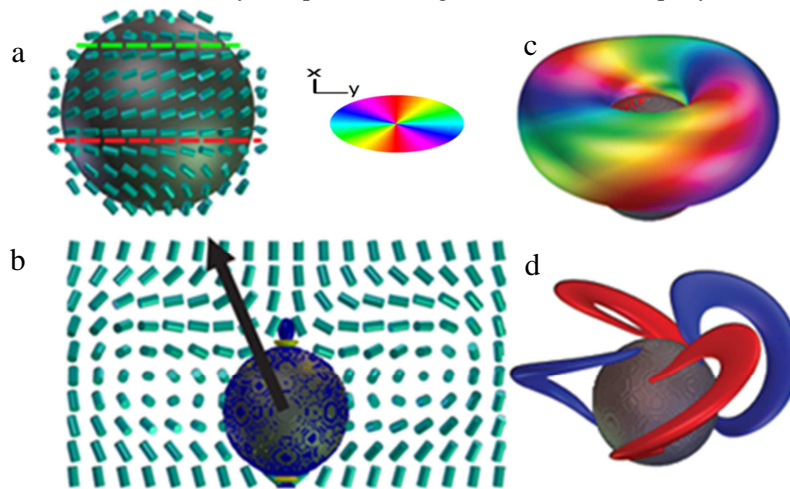


Figure 5: Colloidal particle in the unwinded cholesteric decorated by a hopfion. Director presentations based on (a) glyphs, (b) splay-bend parameter, (c) Pontryagin – Thom surface. (d) Simulated multi-photon fluorescent PM image.

simulated confocal image of multi-photon PM is shown as well. In Figure 6, a cholesteric droplet with homeotropic surface anchoring contains a disclination loop in the form of a trefoil knot: the PT surface is complex and bounded by the disclination loop and the droplet surface.

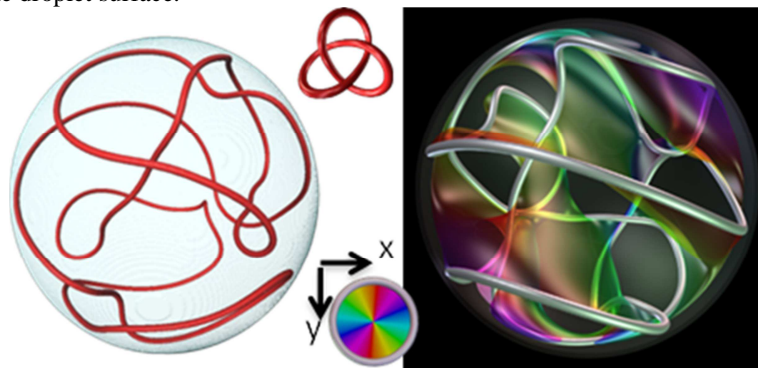


Figure 6: Trefoil knot in a cholesteric droplet with a diameter 5 times the intrinsic pitch. On the right panel a Pontryagin – Thom surface is plotted together with a color wheel describing the director orientation.

3. CONCLUSION

With advances in optical technology and increasing computing power, the resolution and complexity of both experimentally acquired data and simulation results is becoming increasingly higher. To manage the overwhelming amount of raw data, efficient visualisation techniques are an essential part of the research process, as they allow for observation and study of results in an intuitive way, and more easily spot the important features in complex structures. Today multiple state-of-the-art data visualization softwares offer a variety of display methods, including real-time view manipulation, but in order to use them for the particular field of liquid crystals, relevant parameters must first be extracted from the available raw fields. In this brief review, we touched on a broad spectrum of visualization techniques and evaluated their scope of use, advantages and disadvantages. Notably, these approaches can also be combined to show specifically relevant information. For example, combining the splay-bend parameter isosurfaces with order parameter isosurfaces and director glyphs on a cross section is common to achieve a high information density while keeping the maximum readability. Beside the aesthetic appeal, the right choice of a method can uncover hidden structures and lead to a scientific breakthrough. Therefore, keeping up with the current presentation technology should not be neglected.

ACKNOWLEDGEMENTS

This research was financially supported by the Slovenian Office of Science (P1-0099 & Z1-5441). M. R. acknowledges support of FP7 Marie Curie grant FREEFLUID.

REFERENCES

- [1] Tkalec, U., Ravnik, M., Čopar, S., Žumer, S. and Muševič, I., “*Reconfigurable knots and links in chiral nematic colloids*,” *Science* **333**, 62 (2011).
- [2] Smalyukh, I.I., Lansac, Y., Clark, N. and Trivedi, R., “*Three-dimensional structure and multistable optical switching of Triple Twist Toron quasiparticles in anisotropic fluids*,” *Nature Mater.* **9**, 139-145 (2010).
- [3] Chen, B.G., Ackerman, P.J., Alexander, G.P., Kamien, R.D. and Smalyukh, I.I., “*Generating the Hopf fibration experimentally in nematic liquid crystals*,” *Phys. Rev. Lett.* **110**, 237801 (2013).
- [4] Lapointe, C. P., Hopkins, S., Mason, T. G. and Smalyukh, I.I., “*Electrically-driven multi-axis rotational dynamics of colloidal platelets in nematic liquid crystals*,” *Phys. Rev. Lett.* **105**, 178301 (2010).
- [5] Senyuk, B., Liu, Q., He, S., Kamien, R.D., Kusner, R.B., Lubensky, T. C. and Smalyukh, I. I., “*Topological colloids*,” *Nature* **493**, 200-205 (2013).
- [6] Martinez, A., Ravnik, M., Lucero, B., Visvanathan, R., Žumer, S. and Smalyukh, I.I., “*Mutually tangled colloidal knots and induced defect loops in nematic fields*,” *Nature Mater.* **13**, 258 (2014).
- [7] Fukuda, J. and Žumer, S., “*Quasi-two-dimensional Skyrmion lattices in a chiral nematic liquid crystal*,” *Nature Commun.* **2**, 246 (2011).
- [8] Fukuda, J. and Žumer, S., “*Ring Defects in a Strongly Confined Chiral Liquid Crystal*,” *Phys. Rev. Lett.* **106**, 097801 (2011).
- [9] Seč, D., Čopar, S. and Žumer, S., “*Topological zoo of free-standing knots in confined chiral nematic fluids*,” *Nature Commun.* **5**, 3057 (2014).
- [10] Machon, T. and Alexander G.P., “*Knots and nonorientable surfaces in chiral nematics*,” *Proc. Natl. Acad. Sci. USA* **110**, 14174-14179 (2013).
- [11] Ravnik, M. and Žumer, S., “*Landau-de Gennes modelling of nematic liquid crystal colloids*,” *Liq. Cryst.* **36**, 1201 (2009).
- [12] Čopar, S. and Žumer, S., “*Nematic braids: topological invariants and rewiring of disclinations*,” *Phys. Rev. Lett.* **106**, 177801 (2011).
- [13] Alexander, G.P., Chen, B.G., Matsumoto, E.A. and Kamien, R.D., “*Disclination loops, point defects, and all that in nematic liquid crystals*,” *Rev. Mod. Phys.* **84**, 497 (2012).
- [14] Machon, T. and Alexander, G.P., “*Knotted defects in nematic liquid crystals*,” *Phys. Rev. Lett.* **113**, 027801 (2014).

- [15] Čopar, S., Porenta, T. and Žumer, S., “Visualization methods for complex nematic fields,” *Liquid Crystals* **40**, 1759 (2013).
- [16] Trivedi, R.T., Lee, T., Bertness, K.A. and Smalyukh, I.I., “Three dimensional optical manipulation and structural imaging of soft materials by use of laser tweezers and multimodal nonlinear microscopy,” *Opt. Exp.* **18**, 27658 (2010).
- [17] Toulouse, G. and Kléman, M., “Principles of a classification of defects in ordered media,” *J. Phys-Paris.* **37**, 149 (1976).
- [18] Kléman, M., Points, “Lines and Walls: In Liquid Crystals, Magnetic Systems and Various Ordered Media,” John Wiley & Sons Inc., New York (NY), (1982).
- [19] Mermin, N.D., “Topological theory of defects in ordered media,” *Rev. Mod. Phys.* **51**, 591-648 (1979).
- [20] Trebin, H.R., “The topology of nonuniform media in condensed matter physics,” *Adv. Phys.* **31**, 195-254 (1982).
- [21] Kléman, M. and Lavrentovich, O.D., “Soft Matter Physics: An Introduction,” Springer, New York (NY), (2003).
- [22] Kléman, M. and Lavrentovich, O.D., “Topological point defects in nematic liquid crystals,” *Phil Mag.* **86**, 4117-4137 (2006).
- [23] Jänich, K., “Topological properties of ordinary nematics in 3-space,” *Acta Appl. Math.* **8**, 65-74 (1987).
- [24] de Gennes, P.G. and Prost, J., “The Physics of Liquid Crystals,” Oxford University Press, Oxford, (1993).
- [25] Berardi, R., Emerson, A.P.J. and Zannoni, C., “Monte-Carlo investigations of a Gay-Berne liquid-crystal,” *J. Chem. Soc. Faraday Trans.* **89**, 4069-4078 (1993).
- [26] Care, C.M and Cleaver, D.J., “Computer simulation of liquid crystals,” *Rep. Prog. Phys.* **68**, 2665-2700 (2005).
- [27] Smalyukh, I.I, Shiyonovskii, S.V. and Lavrentovich, O.D., “Three-dimensional imaging of orientational order by fluorescence confocal polarizing microscopy,” *Chem. Phys. Lett.* **336**, 88-96 (2001).
- [28] Smalyukh, I.I., Senyuk, B.I., Shiyonovskii, S.V., Lavrentovich, O.D., Kuzmin, A.N., Kachynski, A.V. and Prasad, P.N., “Optical trapping, manipulation, and 3D imaging of disclinations in liquid crystals and measurement of their line tension,” *Mol. Cryst. Liq. Cryst.* **450**, 79-95 (2006).
- [29] Lee, T., Trivedi, R.P. and Smalyukh, I.I., “Multimodal nonlinear optical polarizing microscopy of long-range molecular order in liquid crystals,” *Opt. Lett.* **35**, 3447-3449 (2010).
- [30] Seč, D., Lopez-Leon, T., Nobil, M., Blanc, C., Fernandez-Nieves, A., Ravnik, M. and Žumer, S., “Defect trajectories in nematic shells: Role of elastic anisotropy and thickness heterogeneity,” *Phys. Rev. E* **86**, 020705 (2012).
- [31] Ondris-Crawford, R., Boyko, E.P., Wagner, B.G., Erdmann, J.H., Žumer, S., Doane, J.W., “Microscope textures of nematic droplets in polymer dispersed liquid-crystals,” *J. Appl. Phys.* **69**, 6380-6386 (1991).
- [32] Nych, A., Ognysta, U., Muševič, I., Seč, D., Ravnik, M. and Žumer, S., “Chiral bipolar colloids from nonchiral chromonic liquid crystals,” *Phys. Rev. E* **89**, 062502 (2014).
- [33] Callan-Jones, A.C., Pelcovits, R.A., Slavin, V.A., Zhang, S., Laidlaw, D.H., Loriot, G.B., “Simulation and visualization of topological defects in nematic liquid crystals,” *Phys. Rev. E.* **74**, 061701 (2006).
- [34] Čopar S., Porenta, T. and Žumer, S., “Nematic disclinations as twisted ribbons,” *Phys. Rev. E* **84**, 051702 (2011).
- [35] Čopar, S., Porenta, T., Jampani, V.S.R., Muševič, I. and Žumer, S., “Stability and rewiring of nematic braids in chiral nematic colloids,” *Soft Matter* **8**, 8595 (2012).